CANADA

DEPARTMENT OF
ENERGY, MINES AND RESOURCES
MINES BRANCH
OTTAWA

# *THE MECHANISM OF THE FORMATION OF LEAD HEXAFERRITE*

W. S. BOWMAN, SUTARNO, NORMAN F. H. BRIGHT AND
J. L. HORWOOD

MINERAL SCIENCES DIVISION

Reprinted from the Journal of the Canadian Ceramic Society, (1969), Vol. 38, pp. 1 - 8

*Reprint Series* RS 93

Price 50 cents

© Crown Copyrights reserved

Available by mail from the Queen's Printer, Ottawa
and at the following Canadian Government bookshops

HALIFAX
*1735 Barrington Street*

MONTREAL
*Æterna-Vie Building, 1182 St. Catherine St. West*

OTTAWA
*Daly Building, Corner Mackenzie and Rideau*

TORONTO
*221 Yonge Street*

WINNIPEG
*Mall Center Bldg., 499 Portage Avenue*

VANCOUVER
*657 Granville Street*

or through your bookseller

Price 50 cents Catalogue No. M38-8/93

*Price subject to change without notice*

Queen's Printer for Canada
Ottawa, 1970

# The mechanism of the formation of lead hexaferrite*

W. S. Bowman, Sutarno, Norman F. H. Bright and J. L. Horwood

ABSTRACT. Studies of the mechanism of the formation of lead hexaferrite from its constituent oxides have been conducted. The reactions were studied by differential thermal analysis, thermogravimetric analysis, X-ray diffraction procedures and by magnetic susceptibility measurements. It was found that the nature of the intermediate product(s) was dependent upon the technique of mixing, and the time and temperature of heating. There is an indication that there may be considerable variations in the temperature dependence of the various possible intermediate reactions. A kinetic model describing the behaviour of the system is postulated. The intermediate compounds observed were $2PbO.Fe_2O_3$ and $PbO.2Fe_2O_3$. The latter can be distinguished from the structurally-similar $PbO.6Fe_2O_3$ by the use of magnetic susceptibility measurements.

## Introduction

The group of compounds having the formula $MeO.6{\cdot}0Fe_2O_3$, when Me = Ba and/or Sr and/or Pb, which are commonly known as M-type hexaferrites, are used industrially as the main basic material for ceramic permanent magnets. This type of compound is also one of the basic components of larger hexaferrite-unit structures.

The common method of preparation of these compounds on the industrial scale is by reacting iron oxide with the appropriate Me-carbonate(s). The study of the mechanism of the reactions involved in this formation should, therefore, yield a useful contribution to technology of ferrites.

The purpose of the present investigation was to study the bulk mechanism of the formation of M-type hexaferrites under normal laboratory conditions. Lead hexaferrite was chosen for this work because of the low melting point of lead oxide; this oxide would, consequently, be expected to react with $Fe_2O_3$ at lower temperatures than the more refractory oxides BaO or SrO, thus minimizing the complications due to the sintering of the oxides prior to reaction.

## Experimental techniques

### Sample preparation

**Raw materials.** Reagent grades of lead nitrate, ferric nitrate, iron oxide ($\alpha$-$Fe_2O_3$), ammonium hydroxide and ammonium bicarbonate were used as raw materials without further purification. Both lead and iron nitrates were dissolved in distilled water and the solutions were assayed chemically (1). Experience has shown that there is a slight variation from one batch to the other in both the impurities and in the ferrous-ion content of the iron oxide powder. For this reason the iron oxide powder used for these experiments was analyzed both chemically for the total iron, and spectrographically for its impurity content. The results of these analyses are listed in Table I.

**Co-precipitation method.** Pre-analyzed solutions of lead and ferric nitrates were mixed volumetrically to give the desired molar ratios ($Fe^{3+}/Pb^{2+} = 11.6$ and 12.0). A

W. S. Bowman, Technical Officer; Sutarno, Research Scientist; and Norman F. H. Bright, Head, Physical Chemistry Section; J. L. Horwood, Research Scientist, Solid State Studies Group, all of Mineral Sciences Division, Mines Branch, Department of Energy, Mines and Resources, Ottawa, Canada.

*Presented at the annual meeting of the Canadian Ceramic Society, Electronics Division, Montreal, February 17-18, 1969.

Crown copyright reserved.

*Table I. Semi-quantitative spectrographic analysis of iron oxide used in this work**

| Element | Wt % | Element | Wt % | Element | Wt % | Element | Wt % |
|---|---|---|---|---|---|---|---|
| Ba | ND† | W | ND | Bi | ND | Zn | ND |
| Sr | ND | Pb | ND | Al | 0.006 | Ti | ND |
| Mn | 0.06 | Sn | ND | V | ND | Ni | 0.03 |
| Sb | ND | Cr | ND | Zr | ND | Co | ND |
| Mg | 0.04 | Si | 0.03 | Cu | 0.01 | | |
| Mo | ND | Fe | PC‡ | Ag | ND | | |

*Analysis by D. P. Palombo, *see* Mineral Sciences Division internal report no. MS-AC-68-79, Energy, Mines and Resources, Ottawa.
†ND — non-detectable; PC — principal constituent.
‡The sample was assayed for its total iron content by a chemical method and was found to contain 70.16 Wt % Fe.

25% excess of the amount of crystalline ammonium bicarbonate required to form lead carbonate was dissolved in 1 litre of distilled water. Two litres of the nitrate solution, containing approximately 0.05 mole of lead nitrate and the appropriate amount of iron nitrate, were added drop-by-drop to the ammonium bicarbonate solution. The mixture was stirred vigorously. During the co-precipitation process, the pH was maintained at 8.0 ± 0.1 and the temperature at 65° ± 2°C by adjusting the rate of the feed, the heating and the ammonium hydroxide flow. The resulting slurry was filtered, washed with ethanol and dried overnight at 300°C.

**Semi-co-precipitation (or slurry) method.** Pre-analyzed iron oxide powder was dried at 200°C. A slurry was made by mixing the appropriate amount of lead nitrate solution with a weighed portion of the dried iron oxide to give the desired molar ratios. The concentration of the slurry was approximately the same as that employed in the co-precipitation method. The precipitation of lead in the iron oxide slurry was performed by adding a 25% excess of a solution of ammonium bicarbonate to the slurry. The precipitation was carried out at room temperature and the pH of the slurry was maintained at 8.0 ± 0.1. The resulting mixture was filtered, washed, and dried as before.

In both the co-precipitation and slurry methods, the filtrates were tested after filtering for $Pb^{2+}$ by both chromate and sulphate, and for $Fe^{3+}$ by thiocyanate, in order to ensure that the precipitation was complete.

## TGA, DTA and XRD examinations*

The TGA examinations were conducted in an air atmosphere, using a Stanton Automatic Recording Thermobalance. A recrystallized alumina crucible was used as container. The sample was heated to the required temperature at a rate of 385°C per hour and soaked for up to 2 hours at that temperature. Portions of the sample were withdrawn for XRD examination after soaking times of 0, 1 and 2 hours.

The DTA examinations were conducted in air at a heating rate of 720°C per hour. The standard reference material used was α-alumina. The sample was held in an alumina holder. Pt vs. Pt:13 % Rh thermocouples were used for both sample and differential temperature measurements. The differential EMF and the sample-holder temperature were simultaneously recorded on a two-pen recorder, the former after amplification and the latter directly.

X-ray powder diffraction patterns of the samples, obtained from various stages of the TGA and DTA examinations, were prepared in order to identify the crystalline phases present. Most of the films were obtained with a 114.6-mm-diameter Debye-Scherrer camera, using filtered CoK radiation

*TGA = thermogravimetric analysis; DTA = differential thermal analysis; XRD = X-ray diffraction.

## Magnetic susceptibility measurements

The magnetic susceptibility values of the samples at various heating stages were measured (in arbitrary units) as a change of inductance in a coil that formed one arm of a Wheatstone-bridge circuit. Samples placed within the coil were subjected to very weak, low-frequency (1000 Hz) fields. No evidence of saturation was observed when the driving voltage of the bridge was altered. In order to eliminate the effects of environmental change, an identical coil was used as a reference inductance in the balancing arm of the Wheatstone bridge.

## Experimental results and discussion

The TGA trace of the sample prepared by the co-precipitation method showed that it lost weight until a temperature of about 700°C was reached. For the sample prepared by the slurry method, this weight loss was complete at about 550°C. Both samples began to lose weight again at around 1150°C. The TGA curves are reproduced in Figure 1.

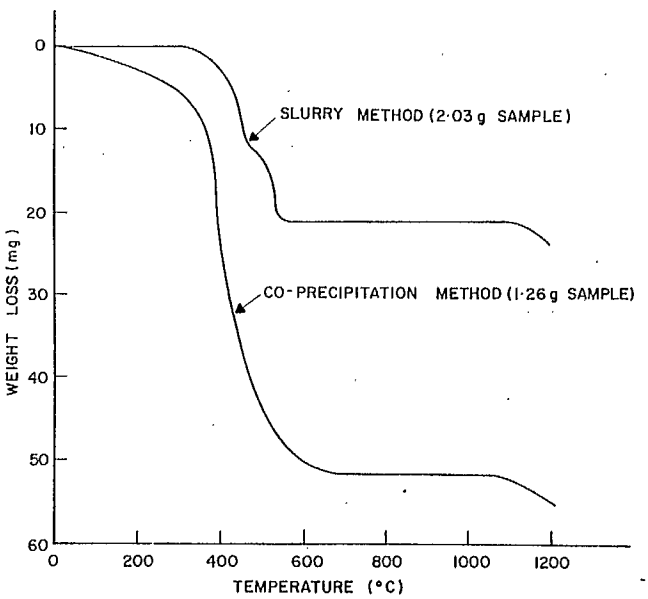


FIGURE 1. TGA curves of the samples prepared by the co-precipitation and slurry methods.

The DTA curves (2) of mixed powders with the $PF_6$* gross composition, prepared by both methods, are reproduced in Figure 2. No attempt has been made to account for all the peaks observed below 500°C. Experience has shown that no hexaferrite XRD pattern can be detected with powders prepared by the above methods on heating up to this temperature (500°C). Above 500°C, for the co-precipitated sample, there is only one endothermic peak, occurring at 665°C. This figure is lower than the Néel point of hematite normally registered at about 680-690°C; in addition, the peak does not exhibit the sharpness of profile normally associated with the Néel peak (3).

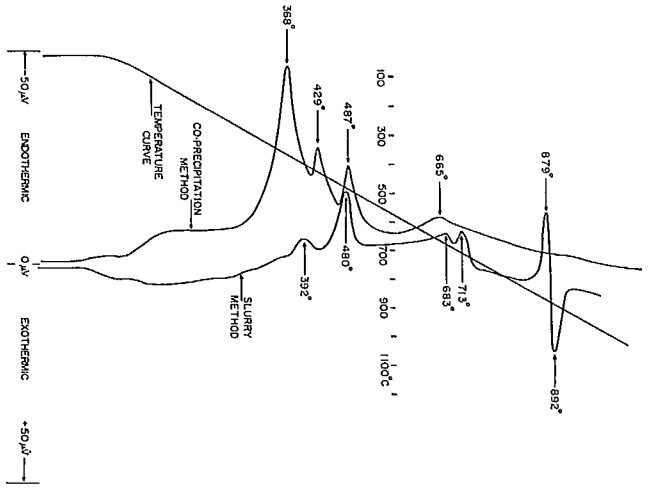


FIGURE 2. The DTA curves of samples with the $PF_6$ composition, prepared by the co-precipitation and slurry methods, previously heated to 300°C.

The slurry sample, on the other hand, shows four peaks at temperatures above 500°C, three of these being endothermic. The first of these peaks occurs at 683°C, and has the characteristic profile of the Néel-point peak of hematite. The second peak occurs at 713°C; the third is a large endothermic peak at 879°C, that is followed immediately by an exothermic peak of about the same size at 892°C.

With the freshly co-precipitated sample, no crystalline material could be detected by XRD analysis. Hence, the form in which the lead was precipitated could not be ascertained by this means. However, the sample, when heated at 200°C, was found to contain lead nitrate and hematite. On further heating, the $Pb(NO_3)_2$ decomposed and, after 1 hour or more at 600°C or higher, a phase having an apparent magnetoplumbite structure began to appear (Table II). The phase diagram of the system $PbO\text{-}Fe_2O_3$(4) shows that the compounds immediately next to $PF_6$ are $PF_2$ on one side and F on the other.

$PF_2$ and $PF_6$ have very similar structures. Figure 3 shows the $PF_6$ structure (5). It has been reported that $PF_2$ has the same basic structure as $PF_6$ with several of the oxygen atoms in the middle plane of the "R" blocks being replaced by lead atoms, with the two octahedrally-coordinated iron atoms associated with this plane missing in order to balance the charges. The two compounds give extremely similar XRD patterns (*see* Table III and Figure 4), and this similarity creates a serious problem in the interpretation of XRD results for the intermediate products. However, there are certain minor lines in the patterns of both $PF_2$ and $PF_6$ that can be considered as diagnostic; these are indicated by arrows on Figure 4. There is no difficulty to diagnose the presence of $P_2F$ by X-ray means.

Table II shows that the formation of $PF_6$ from the co-precipitated sample is virtually complete at about 900°C. The two strongest hematite lines were never completely ab-

*Table II. Phases identified by XRD in samples with $PF_6$ composition prepared by the co-precipitation method after various heat treatments*

| Temperature (°C) | Soaking time (hr) | | |
|---|---|---|---|
| | 0 | 1 | 2 |
| 500 | F + P | F + P | F + P |
| 600 | F + P | F + P + $PF_2$ | F + $PF_2$ + P |
| 700 | F + $PF_2$ + P | F + $PF_2$ + (P) | F + $PF_2$ |
| 725 | F + $PF_2$ | F + $PF_2$ | F + $PF_2$ + $PF_6$ |
| 750 | F + $PF_2$ | F + $PF_2$ + $PF_6$ | F + $PF_2$ + $PF_6$ |
| 775 | F + $PF_2$ + $PF_6$ | F + $PF_6$ + $PF_2$ | F + $PF_6$ + $PF_2$ |
| 800 | F + $PF_6$ + ($PF_2$) | F + $PF_6$ | $PF_6$ + F |
| 900 | $PF_6$ + F | $PF_6$ + (F) | $PF_6$ |
| 1300 | F + ($PF_6$) | | |

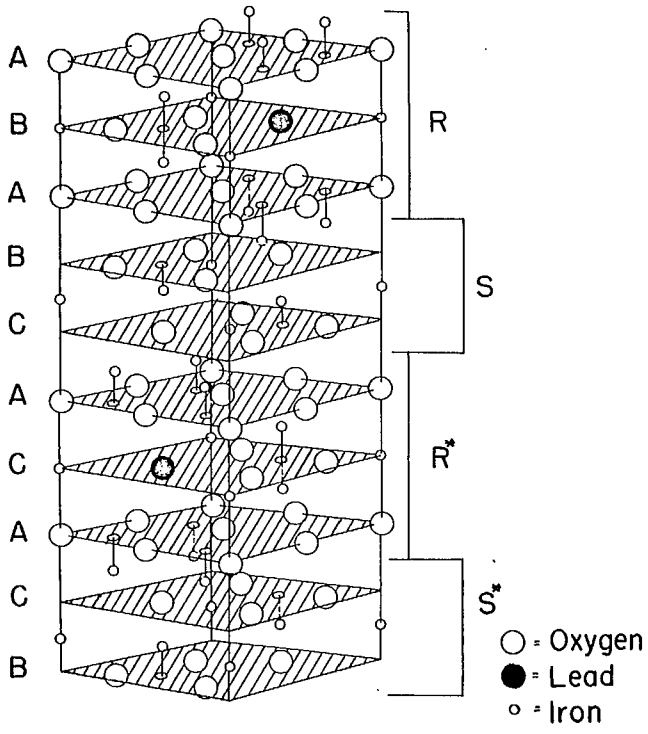


FIGURE 3. Crystal structure of the $PF_6$ compound showing one unit cell.

*P = PbO, F = $Fe_2O_3$, $P_2F$ = 2PbO.$Fe_2O_3$ and $PF_2$ = PbO. 2$Fe_2O_3$ $PF_6$ = PbO.6$Fe_2O_3$. This nomenclature will be used throughout the remainder of this paper.

*Table III. Comparison of X-ray diffraction lines of $PF_2$ and $PF_6$*

| $PF_2$ After Berry (6) | | | Present work Powder with $PF_6$ composition prepared by co-precipitation method. Calcined 600°C 1 hr | | 800°C 0 hr | | $PF_6$ After Mountvala and Ravitz (4) | | |
|---|---|---|---|---|---|---|---|---|---|
| hk*l* | Int. | d(Å) | Int.* | d(Å) | Int.* | d(Å) | hk*l* | Int. | d(Å) |
| 004 | 10 | 11.5 | | | w | 11.9 | | | |
| | | | | | vw | 5.89 | | | |
| 202 | 10 | 5.05 | vw | 5.06 | w | 5.03 | 101 | 30 | 4.97 |
| | | | | | | | 102 | 20 | 4.65 |
| | | | | | vw | 4.27 | 103 | 10 | 4.24 |
| 00 12 | 20 | 3.91 | | | w | 3.88 | 006 | 20 | 3.83 |
| | | | m | 3.68† | m | 3.67† | | | |
| 20 12 | 10 | 3.11 | w | 3.06 | vw | 3.11 | | | |
| 220 | 40 | 2.96 | w | 2.95 | w | 2.95 | 110 | 35 | 2.934 |
| | | | | | vw | 2.86 | 008 | 25 | 2.879 |
| | | | | | w | 2.80 | 112 | 15 | 2.844 |
| 20 14 | 60 | 2.81 | vw | 2.81 | w | 2.76 | 107 | 100 | 2.764 |
| | | | vs | 2.70† | vs | 2.70† | | | |
| 228 | 100 | 2.64 | vw | 2.62 | w | 2.63 | 114 | 85 | 2.618 |
| | | | | | | | 200 | 10 | 2.546 |
| 20 16 | 10 | 2.55 | s | 2.52† | s | 2.51† | 108 | 10 | 2.508 |
| 406 | 20 | 2.44 | vw | 2.43 | vw | 2.43 | 203 | 35 | 2.410 |
| 40 10 | 10 | 2.25 | | | vw | 2.24 | 205 | 25 | 2.227 |
| | | | m | 2.20† | m | 2.20† | | | |
| 22 16 | 5 | 2.09 | vw | 2.07 | vw | 2.07 | 206 | 15 | 2.118 |
| 20 22 | 20 | 1.846 | m | 1.837† | m | 1.838† | 10 11 | 10 | 1.839 |
| | | | | | | | 11 10 | 10 | 1.807 |
| | 5 | 1.732 | | | | | | | |
| 42 14 | 50 | 1.680 | s | 1.691† | s | 1.692† | 217 | 20 | 1.663 |
| 00 28 | 40 | 1.644 | | | | | 00 14 | 10 | 1.649 |

**Visual intensity*: vs–very strong; s–strong; ms–medium strong; m–medium; w–weak; vw–very weak.
†Hematite lines.

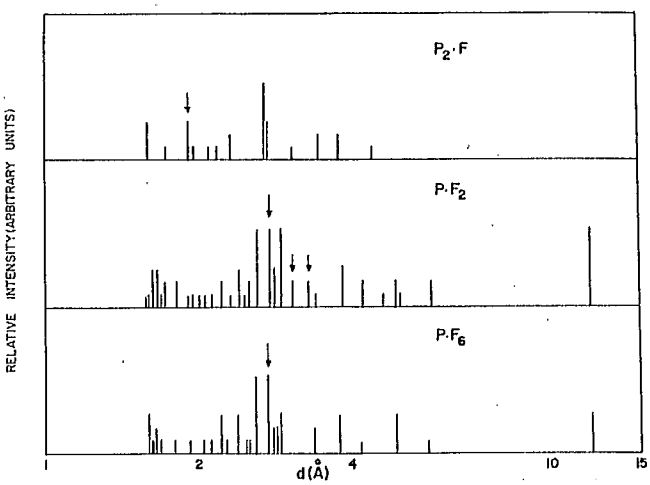


FIGURE 4. Comparison of X-ray diffraction lines of $P_2F$, $PF_2$ and $PF_6$.

sent in the sample with the $PF_6$ composition, but they were extremely weak in samples that had been heated to 900°C or higher. These lines were, however, completely absent in a co-precipitated sample with the $PF_{5.8}$ composition that had been heated at 1100°C. This observation could possibly support the suggestion (7) that the true formula for the "hexaferrites" might be $2MO.11 \cdot 0Fe_2O_3$ rather than $MO.6 \cdot 0Fe_2O_3$. XRD patterns of samples with the $PF_6$ composition heated to above 1150°C showed the presence of considerably more hematite, indicating the loss of some PbO due to volatilization. This is in agreement with the TGA results. By 1300°C, there was very little $PF_6$ remaining.

Fortunately $PF_2$ is anti-ferrimagnetic (4) whereas $PF_6$ is strongly ferrimagnetic. Based on these magnetic properties, the presence of $PF_6$ among the substances giving the magnetoplumbite pattern can be indicated by measurement of their initial magnetic susceptibility. Insertion of a sample into the coil produced typical changes of inductances as follows: (a) before $PF_6$ was formed — 0.003%, (b) after $PF_6$ was formed — 1.5%. These figures are sufficiently different in order of magnitude to give an unequivocal indication of the presence or absence of $PF_6$. Figure 5 shows the initial susceptibility ($\chi_0$) of $PF_6$ compositions plotted against their calcination temperatures. For the sample prepared by the co-precipitation method, $\chi_0$ started to rise from the minimum value at about 660°C. However, the magnetoplumbite-like pattern was detected in this sample at below 600°C. This implies that the substance giving the magnetoplumbite structure below 660°C could, in fact, only be $PF_2$. At 660°C, $PF_2$ started to react with the residual hematite to form $PF_6$. By 775°C, there was enough $PF_6$ formed that, with very careful observation, splitting of

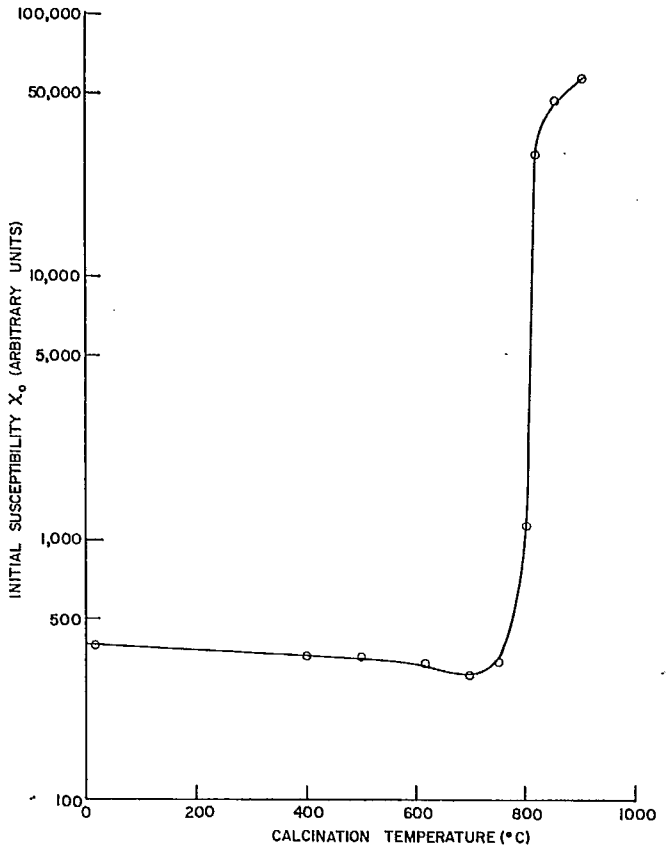


FIGURE 5. Initial magnetic susceptibility of the sample prepared by the co-precipitation method at various calcination temperatures.

(107) lines can be detected, indicating the presence of $PF_6$ and $PF_2$.

The DTA peak at 665°C (*see* Figure 2) is thus associated with the formation of $PF_2$ and its subsequent conversion, by reaction with the residual hematite, to form $PF_6$. It will be seen that the peak is broad, extending over a significant temperature range. The initial formation of $PF_2$ is indicated from Table II as taking place at 600°C in the samples heated for 1 or 2 hours. The DTA trace, however, shows its peak at 665°C. It is entirely reasonable that the soaking experiments, being static and extending over significant time intervals, should record the reaction as occurring at a detectable rate at lower temperatures than are observed in the DTA technique, in which the reaction is studied under dynamic conditions whereby the sample temperature is constantly changing. It is thought probable that most of the enthalpy change associated with this peak is due to the formation of $PF_2$ since only a slight structural change is involved in going from $PF_2$ to $PF_6$; this slight change would, presumably, be associated with only a very small enthalpy effect.

The situation is quite different with the samples prepared by the slurry method. Figure 2 shows that there was considerably more thermal activity in this sample than in the co-precipitated sample. With the slurry sample, the lead compound present after heating the sample to 300°C could not be identified by XRD. When the sample was heated to 700°C, without soaking, the lead salt decomposed into PbO without reacting with the hematite (*see* Table IV). In Figure 2, the Néel-point peak of hematite is very clear in the sample prepared by the slurry method, but is absent in the co-precipitated sample. No lead-iron compound was detected at temperatures below 700°C; on heating at this temperature or higher for 1 hour or more, the compound $P_2F$ started to form.

*Table IV. Phases identified by XRD in samples with $PF_6$ composition prepared by the slurry method after various heat treatments*

| Temperature (°C) | Soaking time (hr) | | |
|---|---|---|---|
| | 0 | 1 | 2 |
| 700 | F + P | F + P + ($P_2F$) | F + $P_2F$ + P |
| 750 | F + P + ($P_2F$) | F + $P_2F$ | F + $P_2F$ |
| 800 | F + $P_2F$ | F + $P_2F$ | F + $P_2F$ |
| 825 | F + $P_2F$ | F + $P_2F$ | F + $P_2F$ |
| 850 | F + $P_2F$ | F + $PF_6$ + $P_2F$ | $PF_6$ + F + ($P_2F$) |
| 900 | F + $PF_6$ + ($P_2F$) | $PF_6$ + F | $PF_6$ + F |
| 1000 | $PF_6$ + F | $PF_6$ + F | $PF_6$ + (F) |
| 1300 | F + $PF_6$ | | |

Table V shows a comparison of XRD patterns of $P_2F$ and of the intermediate product in the formation of $PF_6$ in the slurry method. The DTA peak observed at 713°C may be associated with the formation of the $P_2F$ compound. This compound becomes a major constituent and subsequently melts at a temperature of 879°C. This melting accounts for the large endothermic DTA peak at this temperature. Evidence for this statement was found by preparing the compound $P_2F$ by the co-precipitation method with calcination at 800°C without soaking (Table V). This sample melted at 879°C when it was examined by DTA. Also, the DTA curve obtained from a sample with the $PF_6$ composition, prepared by dry-mixing $P_2F$ and commercial $Fe_2O_3$ (the same as was used in the slurry method), was almost identical with the curve obtained from the sample prepared by the normal slurry method.

The magnetic susceptibility measurements (*see* Figure 6) show that $\chi_o$ started to rise from its minimum value at about 700°C. However, owing to the much lower sensitivity to the detection of minor constituents, no magnetoplumbite structure was detectable by XRD until a substantially higher temperature was reached. The formation of $PF_6$ in this sample was, therefore, a result of the reaction between $P_2F$ and F. From the above evidence, it appears that the reaction

$$P_2F + 11F \rightarrow 2PF_6 \quad \text{(Eq. 1)}$$

is a solid-solid reaction in the initial stages followed by a solid-liquid reaction, corresponding to the peak at 892°C. The formation of $PF_6$ was not complete until a temperature of about 1000°C was reached. There was no evidence either to support or to deny that the formation of $PF_2$ can occur simultaneously with that of $PF_6$. As with the co-precipitated sample, the hexaferrite prepared by the slurry method began to lose PbO by volatilization at about 1150°C.

*Table V. Comparison of diffraction lines of $P_2F$ and of the intermediate product in the formation of $PF_6$ by the slurry method*

| | | | Present work | | | | | |
|---|---|---|---|---|---|---|---|---|
| | | | Powder with $PF_6$ composition prepared by slurry method Calcined | | | | Powder with $P_2F$ composition prepared by co-precipitation method Calcined | |
| | $P_2F$ calculated from Berger and Pawlek (8) | | 700°C 2 hr | | 850°C 0 hr | | 800°C 2 hr | |
| hkl | Int. | d(Å) | Int.* | d(Å) | Int.* | d(Å) | Int.* | d(Å) |
| | | | vw | 5.93‡ | | | | |
| 112 | 5 | 4.53 | vw | 4.51 | w | 4.47 | vw | 4.53 |
| 004 | 14 | 3.98 | | | | | | |
| 200 | 23 | 3.88 | w | 3.87 | m | 3.85 | w | 3.86 |
| | | | m | 3.68† | m | 3.67† | | |
| 104, 202 | 13 | 3.53 | vw | 3.54 | | | w | 3.52 |
| | | | m | 3.05‡ | | | | |
| | | | w | 2.94‡ | | | | |
| 220 | 100 | 2.77 | s | 2.76 | vs | 2.77 | m | 2.78 |
| 204 | | | | | | | | |
| | | | vs | 2.70† | vs | 2.69† | | |
| | | | s | 2.52† | s | 2.51† | | |
| 116 | 2 | 2.39 | | | | | | |
| 312 | 9 | 2.36 | w | 2.36 | w | 2.35 | w | 2.35 |
| 313, 206 | 3 | 2.20 | m | 2.21† | m | 2.20† | vw | 2.20 |
| 321 | 1 | 2.14 | vw | 2.08† | vw | 2.07† | vw | 2.13 |
| 008 | 13 | 1.985 | vw | 1.999 | vw | 1.987 | vw | 1.976 |
| 400 | 22 | 1.950 | w | 1.945 | m | 1.947 | m | 1.946 |
| | | | m | 1.840† | m | 1.839† | | |
| 208 | 11 | 1.769 | vw | 1.795 | vw | 1.742 | vw | 1.743 |
| 404, 420 | | 1.747 | vw | 1.718 | | | | |
| | | | m | 1.691† | m | 1.693† | | |
| | | | vw | 1.637† | | | | |
| 228 | 41 | 1.613 | | | | | | |
| 424 | | 1.597 | w | 1.596 | m | 1.597 | ms | 1.596 |
| | | | vw | 1.532 | | | | |
| | | | m | 1.483† | m | 1.483† | | |
| | | | vw | 1.468 | | | | |
| | | | m | 1.452† | m | 1.451† | | |
| 408 | 9 | 1.391 | | | | | | |
| 440 | 9 | 1.379 | | | | | m | 1.376 |
| 620, 604 | 11 | 1.234 | | | | | m | 1.231 |

**Visual intensity*: vs–very strong; s–strong; ms–medium strong; m–medium; w–weak; vw–very weak.
†Hematite lines.
‡PbO lines

## Theoretical considerations

From the above results, there are apparently two different mechanisms for the formation of $PF_6$ from its oxide components. The occurrence of the various phases over the relevant ranges of temperature is illustrated schematically in Figure 7. It is difficult to believe that the production of different intermediate products by the two different processes, indicating two different mechanisms of reaction, could be attributable to real thermodynamic differences. It is more reasonable to consider that these differences are of a kinetic nature, and that some simple model can be postulated to explain both mechanisms.

Let us assume that the formation of $PF_6$ from the oxide components proceeds via the following steps:

$$2P + 12F \underset{}{\overset{K_1}{\rightleftarrows}} P_2F + 11F \overset{K_2}{\rightleftarrows} 2PF_2 + 8F \overset{K_3}{\rightleftarrows} 2PF_6 \ldots \text{(Eq. 2)}$$

where $K_1$, $K_2$ and $K_3$ are the rate constants for the first, second and third steps of the reaction, respectively.

These three rate constants will, in general, depend to different extents upon temperature, i.e., the Arrhenius plots of log K against 1/T will have different slopes. Assuming that the plots of log $K_1$, log $K_2$, and log $K_3$ against 1/T intersect within the temperature range covered by the experimental formation of the compounds $P_2F$, $PF_2$ and $PF_6$, then it is possible to select gradients for the three log K vs. 1/T plots which will be consistent with the experimental observations of the occurrence or non-occurrence of any particular compound at any temperature within the range under consideration.

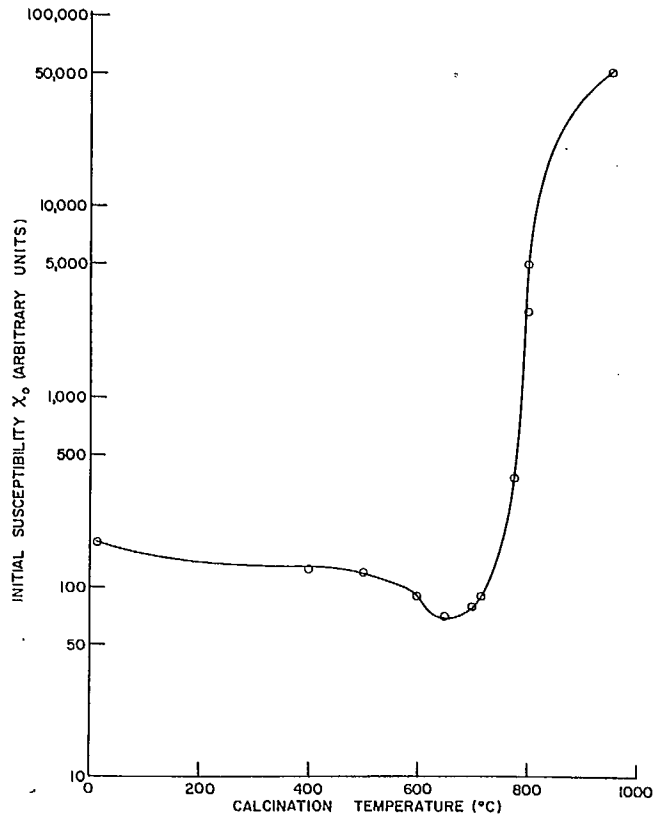


FIGURE 6. Initial magnetic susceptibility of the sample prepared by the slurry method at various calcination temperatures.

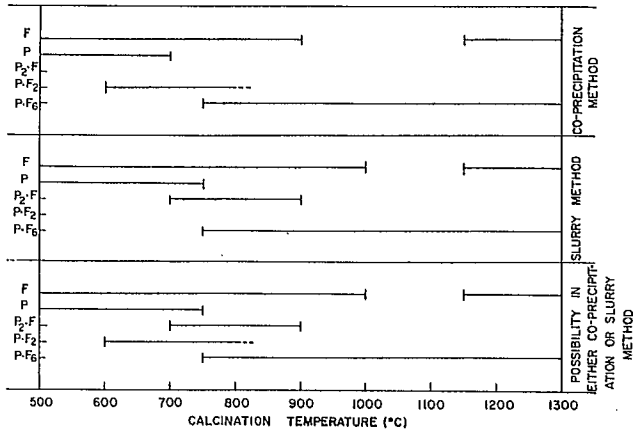


FIGURE 7. Calcination-temperature ranges over which the various compounds are observed.

If we consider first the stages $K_3$ and $K_2$, then, if the log $K_3$ plot is steeper than the log $K_2$ plot, at relatively low temperatures $PF_3$ and $PF_6$ will be observed but not $P_2F$, whereas, at relatively high temperatures, $P_2F$ and $PF_6$ will be observed but not $PF_2$. As will be seen from Figure 7 and Tables II and IV, the reaction to form $PF_6$ occurs at a higher temperature with the slurry method than with the co-precipitation method. This accords with above postulates. Similar types of consideration can be developed for the $K_1$—$K_2$ relationships with temperature. In this case, in order to be consistent with the observed facts, the plot of log $K_1$ vs. 1/T must be steeper than that of log $K_2$.

The experimental verification of the above postulates concerning the relative dependences of $K_1$, $K_2$ and $K_3$ on temperature could be achieved by measurement of diffusion rates of PbO into $Fe_2O_3$ or vice versa in a composite PbO/$Fe_2O_3$ pellet heated at various temperatures. It is hoped to conduct experiments along these lines. If these postulates are, in fact, verified, then it still remains to explain *why* the rates should depend differently upon temperature and to work out how the relative particle sizes of the reacting species will affect the absolute values of these rates, taking into consideration such factors as areas of contact, whether the reaction occurs by solid-solid interaction or by vapour-phase diffusion, and whether a liquid phase is involved at any stage. This also it is hoped to do.

Apparently the kinetic differences in the mechanism of the formation of $PF_6$ between the samples prepared by the co-precipitation and by the slurry methods are, indeed, associated in some way with differences in average particle size of the iron oxides used in the two samples. The results of the following test would indicate this. Hydrated $Fe_2O_3$ was precipitated from an iron nitrate solution. The precipitate was collected and dried thoroughly at 200°C. Part of it was then calcined at 800°C to ensure complete dehydration. $PF_6$ compositions were prepared by dry-mixing PbO (yellow) with portions of both the calcined and the uncalcined iron oxide. The two mixtures were then heated to 800°C. XRD patterns showed the formation of $P_2F$ in the sample prepared using calcined $Fe_2O_3$ and of $PF_2$ in the sample prepared using uncalcined $Fe_2O_3$. The surface area of the calcined iron oxide was 3.4 $m^2/g$ and of the uncalcined, 113.9 $m^2/g$. Such differences could well be kinetically significant.

All that has been achieved at the present stage of the investigation is to indicate that there are two different mechanisms of the formation of $PF_6$ from its constituent oxides, that the intermediate products are either $P_2F$ or $PF_2$, depending on circumstances, and that there is a logical kinetic pattern which is consistent with these experimental observations.

## Conclusions

1. The experimental conditions selected (pH, temperature and quantity of carbonate used) are sufficient to ensure the complete precipitation of both iron and lead. However, the form in which the lead was precipitated could not be identified by X-ray diffraction.

2. Magnetic susceptibility measurements were found to be more sensitive than XRD as a means of detecting the existence of a magnetic compound in the non-magnetic matrix (in this case, the presence of $PF_6$ in a matrix of $PF_2$). This experimentally simple method was a very useful tool to study the reaction mechanisms in the PbO-$Fe_2O_3$ system.

3. There is an apparently different reaction mechanism for the formation of $PF_6$ when prepared by co-precipitation from when prepared by the slurry method. The former method gave $PF_2$ as its intermediate product, whereas in the

second, $P_2F$ was observed as the intermediate product. In both cases the reactions were complete at about 1000°C.

4. It is probable that this difference is not of a thermodynamic nature but rather a kinetic phenomenon. Further experiments are in hand to clarify this point.

## Acknowledgments

The authors are indebted to Dr. A. H. Webster for valuable discussions throughout the investigation. Thanks are also due to Mr. E. J. Murray and Mr. P. E. Porteous for preparing XRD charts and films, and to Mr. R. H. Lake for preparing DTA and TGA charts. The above personnel are all members of the staff of the Mineral Sciences Division, Mines Branch, Department of Energy, Mines and Resources.

This investigation was conducted in the Physical Chemistry Section, Mineral Sciences Division, Mines Branch and was partly supported by Defence Research Board Contract ECRDC C-73 under the co-ordination of Mr. I. F. Wright, Mineral Processing Division, Mines Branch.

The authors also wish to thank Dr. T. R. Ingraham, Extraction Metallurgy Division, Mines Branch, for helpful discussions of the kinetic aspects of this problem.

## References

1. Vogel, A. I. Quantitative inorganic analysis. John Wiley, New York, 1961, pp. 468-472 and 484.
2. McAdie, H. G. Recommendations for reporting thermal analysis data. *Anal. Chem., 39:* 543, 1967.
3. Schneider M. et Beaulieu, C. E. Transformation du second ordre dans $Fe_2O_3$ à 685°C. *Can. Met. Quart., 6*(1): 1-7, 1967.
4. Mountvala, A. J. and Ravitz, S. F. Phase relations and structures in the system PbO-$Fe_2O_3$. *J. Am. Ceram. Soc., 45*(6): 286-288, 1962.
5. Smit, J. and Wijn, H. P. J. Ferrites. John Wiley, New York, 1959, pp. 182-183.
6. Card Number 9-48, Powder Diffraction File, *Am. Soc. Testing Mater.*
7. Anderson, J. S. Oxford Univ., England, (personal communication).
8. Berger W. and Pawlek, F. Kristallographische und magnetische Untersuchungen im System Bleioxyd (PbO)-Eisenoxyd ($Fe_2O_3$). *Arch. Eisenhüttenw., 28*(2): 101-108, 1957.